Effect of the Specific Pressing Force, Material Moisture Content and Roll Speed on Throughput of the High-Pressure Grinding Roll: Pilot-Scale Test on Copper Mountain Mine Ore, South-Central British Columbia (Part of NTS 92H/07)

G. Pamparana[1], **Norman B. Keevil Institute of Mining Engineering, The University of British Columbia, Vancouver, British Columbia, giovannipamparana@gmail.com**

B. Klein, Norman B. Keevil Institute of Mining Engineering, The University of British Columbia, Vancouver, British Columbia

M.G. Bergerman, Department of Mining and Petroleum Engineering, University of São Paulo, São Paulo, Brazil

Pamparana, G., Klein, B. and Bergerman, M.G. (2024): Effect of the specific pressing force, material moisture content and roll speed on throughput of the high-pressure grinding roll: pilot-scale test on Copper Mountain mine ore, south-central British Columbia (part of NTS 92H/07); *in* Geoscience BC Summary of Activities 2023, Geoscience BC, Report 2024-01, p. 67–78.

Introduction

High-pressure grinding roll (HPGR) technology has gained significant attention for the comminution of hard ores, primarily due to its energy efficiency compared to traditional autogenous (AG) and semi-autogenous grinding (SAG) mill circuits. Studies have demonstrated that HPGR circuits can decrease energy requirements by 10 to 40% (Schönert, 1988; Morell, 2022). Moreover, HPGR comminution also presents downstream benefits, such as improved mineral liberation and reduced particle strength, due to the creation of microfractures along grain boundaries (Ghorbani et al., 2013).

Manufacturers usually perform a series of pilot-scale HPGR tests to obtain the required information to set the standard parameters for industrial use (Rashidi et al., 2017). Pilot-scale testing can also be used to evaluate the performance of the HPGR under different operating conditions, allowing the development of models for purposes such as circuit simulation.

The optimal operation of HPGRs is essential to achieving the desired particle size reduction and product quality while minimizing energy consumption and operating costs. However, achieving the optimal operation of HPGRs can be challenging due to the complexity of the comminution process and the interaction between different operational variables, including properties of the feed material—such as the moisture content—the operating pressure, and the roll speed.

In 2008, a pilot-scale HPGR unit manufactured by the Köppern Group of Hattingen, Germany, was installed at the Coal and Mineral Processing Laboratory of the Norman B. Keevil Institute of Mining Engineering at The University of British Columbia (UBC) in Vancouver, British Columbia. Over the last 15 years, more than 200 pilot-scale tests were performed with this unit on materials from a range of mineral deposits to assess HPGR comminution, determine design parameters for industrial-scale units, and support academic research.

The aim of this study is to investigate the usefulness of HPGR pilot-scale tests in understanding the relationship between operational variables. A ‘design of experiments’ (DOE) approach was employed, varying the pressing force, roll speed, and moisture content of the feed material, to determine their impact on the product size distribution, specific energy consumption, and overall performance of the HPGR.

Methodology

Test Facility and Set Up

The Köppern pilot-scale HPGR installed at UBC (Figure 1) was used to conduct the pilot-scale testing for this study. The rolls of the pilot unit have a Hexadur® liner, a diameter of 0.75 m, and a width of 0.22 m. Material to be tested is choke-fed into the unit from a feed hopper located above the rolls. The machine is equipped with a variable-speed drive and a hydraulic system that can apply a pressing force of up to 8 newtons per square millimetre (N/mm^2). The HPGR programmable logic controller is connected to several sensors that record information from each test through a data-logger for data analysis, including the roller gap, applied pressure, power draw, torque, roll speed and testing time. Table 1 shows the specifications of the installed pilot-scale HPGR unit at UBC.

[1] *The lead author is a 2023 Geoscience BC Scholarship recipient.*

This publication is also available, free of charge, as colour digital files in Adobe Acrobat® PDF format from the Geoscience BC website: https://geosciencebc.com/updates/summary-of-activities/.

Figure 1. Photos of the Köppern pilot-scale high-pressure grinding roll (HPGR) unit installed at The University of British Columbia: **left)** the pilot-scale HPGR unit; **right)** close-up of the HPGR roll's liners.

Table 1. Specifications for the components of the Köppern pilot-scale high-pressure grinding roll unit installed at The University of British Columbia. Abbreviations: kN, kilonewtons; kW, kilowatts; N, newtons; rpm, revolutions per minute.

Component	Value
Roll diameter	0.75 m
Roll width	0.22 m
Press drive	Dual output shaft gear reducer
Feed system	Gravity
Wear surface (roll liner)	Hexadur® WTII
Installed power	200 kW
Maximum pressing force	1600 kN
Maximum specific pressing force	8.5 N/mm^2
Static gap	9 mm
Variable speed drive	Up to 40 rpm (1.55 m/s)

Table 2. The three operational factors considered in the design of experiments for the pilot-scale high-pressure grinding roll tests, and the levels at which they were tested. Abbreviations: Max., maximum; Min., minimum; N, newtons.

Letter designator	Operational factor	Units	Min.	Max.	Mean	Standard deviation
A	Force	N/mm^2	2.5	4.5	3.5	0.79
B	Roll speed	m/s	0.35	0.75	0.55	0.12
C	Moisture content	%	2.5	6	4.43	1.4

Testing Material

Ore from the Copper Mountain mine near Princeton, in the southern interior of British Columbia, was supplied for HPGR testing. Approximately 5 t of material, from the same geometallurgical unit, was collected from Copper Mountain's SAG mill feed, which had been previously crushed with a gyratory crusher and a cone crusher. Once at UBC, the material was screened and crushed to a maximum particle size of 32 mm, then homogenized and split using a rotary splitter.

A complete exploratory analysis comprising 17 pilot-scale tests was performed on the material. Each pilot-scale HPGR test was run using approximately 300 kg of sample. The moisture content was adjusted and homogenized immediately before each test to avoid segregation of the moisture and evaporation.

Experimental Program Design

For the HPGR, three operational factors can influence comminution: A—the specific pressing force, B—the roller speed, and C—the moisture content of the material being pressed. For the pilot-scale HPGR, these three variables can be changed relatively easily for each pilot run, allowing a controlled study of how each factor affects the responses of interest.

A custom DOE was developed to assess the effect of the three operating factors. Table 2 shows these three factors and the levels at which they were tested.

For each pilot-scale HPGR test, samples weighing at least 250 kg are required, therefore a total of 17 pilot-scale HPGR tests could be performed with the available material. The experimental design was developed so that most combinations of operational factors and levels could be tested, prioritizing assessing the specific pressing force thoroughly. Table 3 shows the combination of tested variables for each of the 17 tests carried out. Table 3 shows the levels of the factors tested as codes, where –1 corresponds to the minimum level tested for each factor, 0 corresponds to the mean level, and 1 corresponds to the maximum level, as specified in Table 2. Coding the levels of the variables allows for an easy and direct analysis of the effect of each factor independently of their scale.

Each of the 'blocks' shown in Table 3 corresponds to a different part of the experimental design, and each 'block' of tests focuses on different variables. Block 1 is a two-factor DOE, varying the pressing force and roll speed while main-

Table 3. Details of the complete experimental design, showing the coded factor levels for each test run, where –1 is the minimum level tested for that factor, 0 is the mean level, and 1 is the maximum level. Each 'DOE block' corresponds to a separate experimental design, in which one of the factors is fixed. Abbreviations: DOE, design of experiments; N, newtons.

Test no.	DOE block no.	Factor A Force (N/mm^2)	Factor B Roll speed (m/s)	Factor C Moisture content (%)
1	1	-1	-1	-1
2	1	1	-1	-1
3	1	-1	1	-1
4	1	1	1	-1
5	1	0	0	-1
6	1	0	0	-1
7	1	0	0	-1
8	2	-1	0	-1
9	2	1	0	-1
10	2	0	-1	-1
11	2	0	1	-1
12	3	0	0	1
13	3	0	0	0
14	3	-1	0	1
15	3	1	0	0
16	3	1	0	1
17	3	-1	0	0

taining the moisture content at a typical HPGR operational level (2.5% moisture content). This block contains three repeats at mean values (runs 5 to 7) to assess for response variability. Block 2 enhances block 1, testing mean levels of the pressing force and roll speed. Block 3 is another two-factor DOE that varies the pressing force and moisture content while maintaining the roll speed at a typical testing level (0.55 m/s), which expands the testing at mean levels. It must be noted that runs 8 and 9 of test block 2 also include this two-factor design but were not repeated due to limited material availability.

Responses Tested in the Experimental Program

The following eight responses were recorded during each of the 17 test runs:

1) Average operating gap (mm)
2) Specific energy consumption (kWh/t)
3) Throughput (t/h)
4) Specific throughput, or m-dot (tonnes per hour per cubic metre per second [ts/hm^3])
5) Reduction ratio of 50%
6) Reduction ratio of 80%
7) Flake density (g/cm^3)
8) Flake thickness (mm)

The operating gap is the distance between the rolls when no pressure is applied. It is a critical parameter that affects the product particle size distribution. The specific energy consumption is the amount of energy required to comminute a unit of ore and is an indicator of the circuit's energy efficiency. Throughput is the amount of material processed by unit of time, whereas the specific throughput is the material processed per unitary roll dimensions (a roll of 1 m diameter, 1 m width and rolling at 1 m/s). Both are essential for circuit design and optimization. The 80% and 50% reduction ratios refer to the ratio between the feed (F_{80} or F_{50}) and the product (P_{80} or P_{50}; particle size at which 80% or 50% of the material will pass when screened), indicating the degree of particle size reduction. Flake density and thickness are measured directly from the flakes collected during the HPGR operation. They represent the physical characteristics of the HPGR product and are related to the product size distribution and properties of the ore.

By measuring these particular responses, a holistic view of the HPGR process can be obtained, enabling the identification of optimal conditions for operation and the development of predictive models for scale-up and simulation.

Results

Results From the Experimental Design

The results from the 17 pilot-scale HPGR tests performed are summarized in Table 4.

Each of the eight responses recorded during the test runs was modelled individually, to study how each variable affects the operation and outcome of the HPGR. For this study, an initial quadratic model was considered, and then, using the p-value criterion, an elimination process was performed to develop the final model. An 'analysis of variance' was performed on the resulting model to assess the significance of each predictor and the model and if the lack of fit was significant. The resulting coded coefficients and p-values are summarized in Table 5.

The coded coefficients are useful for directly comparing the influence of each predictor over the ranges of predictor levels tested since they are all on the same scale (–1, 0 and 1), meaning that the larger the absolute value of the coded coefficient, the more significant the effect of the predictor on the response (either positive or negative). A model term is considered significant if the p-value is less than 0.05, whereas p-values over 0.1 are considered not significant for the model. The model terms included in the final model with p-values over 0.1 support hierarchy due to interactions or quadratic terms present that include them.

Analysis of the Results of the Experimental Program

Operating Gap

Figure 2 shows how the three operational factors affected the operating gap. As expected, the specific pressing force has the most significant effect. A higher applied force will generate a larger compression of the material and, thus, reduce the operating gap. The second largest effect is the moisture content, significantly reducing the operating gap as the moisture content increases. Increased moisture contents can lubricate the physical particle interactions, reducing the overall strength of the particle bed and enabling the gap to collapse. The roll speed has the lowest effect, where an increase reduces the gap.

Specific Energy Consumption

Figure 3 shows how the three operational factors affect the specific energy consumption. Optimizing energy consumption to obtain the best particle size reduction using the least energy possible is of great interest. As expected, increasing the specific pressing force increases the specific energy consumption due to an increase in the machine's

Table 4. Summary of the results of the pilot-scale high-pressure grinding roll tests. Abbreviations: kWh/t, kilowatt-hours per tonne; N, newtons; RR, reduction ratio; t/h, tonnes per hour; ts/hm^3, tonnes per hour per cubic metre per second.

Test no.	Factor A Force [N/mm^2]	Factor B Roll speed [m/s]	Factor C Moisture content [%]	Operating gap [mm]	Specific energy [kWh/t]	Throughput [t/h]	Specific throughput [ts/hm^3]	RR_{80}	RR_{50}	Flake density [g/L]	Flake thickness [mm]
1	2.5	0.35	2.5	22.5	1.51	15.8	268.4	2.39	3.09	2.39	27.4
2	4.5	0.35	2.5	19.9	2.64	14.3	243.3	3.33	4.37	2.39	24.7
3	2.5	0.75	2.5	21.7	1.53	31.6	253.4	2.41	3.39	2.39	25.6
4	4.5	0.75	2.5	19.1	2.71	29	231.8	3.34	4.57	2.39	23.9
5	3.5	0.55	2.5	21.8	1.95	23.8	256.6	3	4.03	2.39	26.2
6	3.5	0.55	2.5	21.4	1.97	23.3	252.5	3.04	3.76	2.38	25.4
7	3.5	0.55	2.5	20.3	2.09	22.8	247.3	2.9	3.49	2.38	25.4
8	2.5	0.55	2.5	21.8	1.49	23.9	258.6	2.46	3.73	2.38	27.4
9	4.5	0.55	2.5	19.4	2.68	21.8	236.9	3.28	4.59	2.38	23.5
10	3.5	0.35	2.5	21.1	2.03	14.8	253.6	3.13	4.42	2.36	25.9
11	3.5	0.75	2.5	19.9	2.12	29.7	237.8	3.08	4.24	2.39	23.8
12	3.5	0.55	6	18.5	2.5	21.8	236.6	2.95	4.34	2.32	22.7
13	3.5	0.55	4.25	19.6	2.27	22.5	244.6	2.85	3.51	2.35	24.7
14	2.5	0.55	6	20.3	1.66	23.6	256.5	2.45	3.23	2.37	25
15	4.5	0.55	4.25	17.7	3.02	20.4	220.2	3.51	4.36	2.33	21.9
16	4.5	0.55	6	16.6	3.1	20	219.8	3.22	4	2.31	20.4
17	2.5	0.55	4.25	21.4	1.55	24.1	260.9	2.71	3.95	2.35	26.7

Table 5. Summary of the coded linear regression (intercept and coefficients) and p-values for each of the eight responses measured in the pilot-scale tests. Factor A is the specific pressing force, factor B is the roll speed, and factor C is the moisture content.

Response	Intercept	Factor A	Factor B	Factor C	Factor A x factor C
Operating gap	19.65	-1.51	-0.46	-1.07	
p-values		*< 0.0001*	*0.03*	*0.02*	
Specific energy consumption	2.23	0.67		0.14	0.08
p-values		*< 0.0001*		*0.03*	*0.02*
Throughput	22.25	-1.51	7.57	-0.53	-0.44
p-values		*< 0.0001*	*< 0.0001*	*0.21*	*0.04*
Specific throughput	243.52	-16.26	-7.06	-4.25	-4.17
p-values		*< 0.0001*	*0*	*0.17*	*0.01*
Reduction ratio 80%	2.95	0.43			
p-values		*< 0.0001*			
Reduction ratio 50%	3.99	0.45			
p-values		*0*			
Flake density	2.36	-0.02		-0.01	-0.02
p-values		*0*		*0.13*	*0*
Flake thickness	23.88	-1.77	-0.77	-1.73	
p-values		*< 0.0001*	*0.01*	*0.01*	

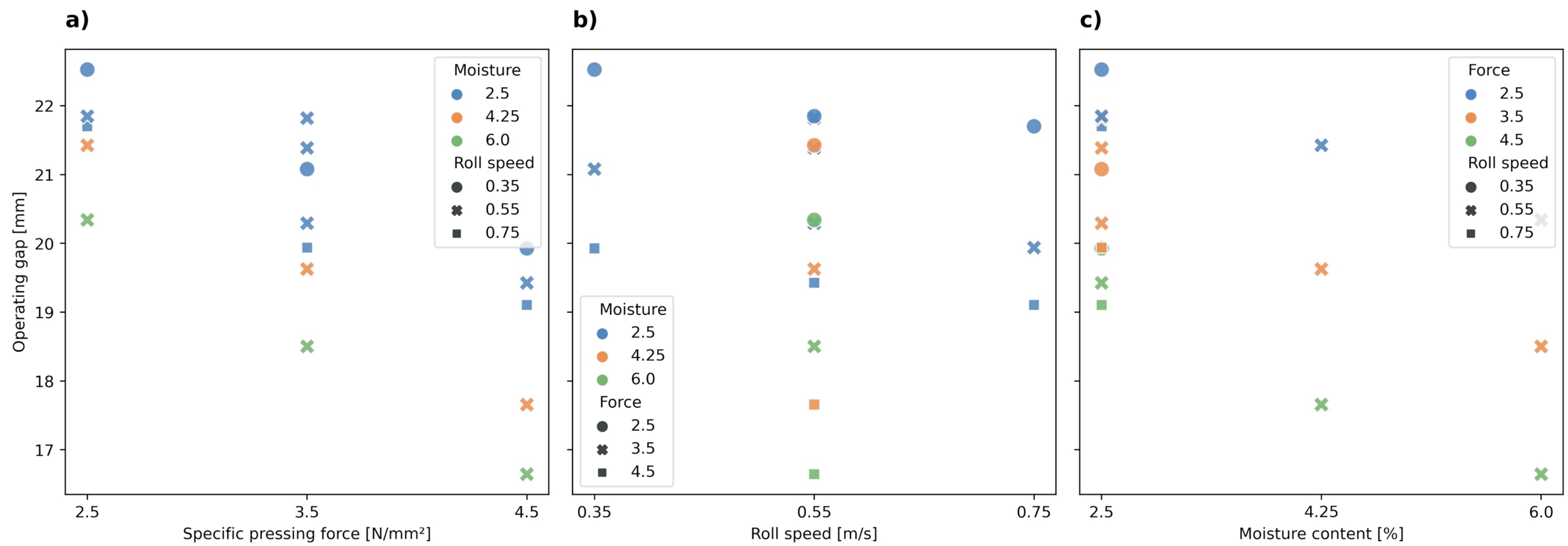

Figure 2. Effect of the operational factors—**a)** specific pressing force, **b)** roll speed, and **c)** moisture content—on the operating gap. Abbreviation: N, newtons.

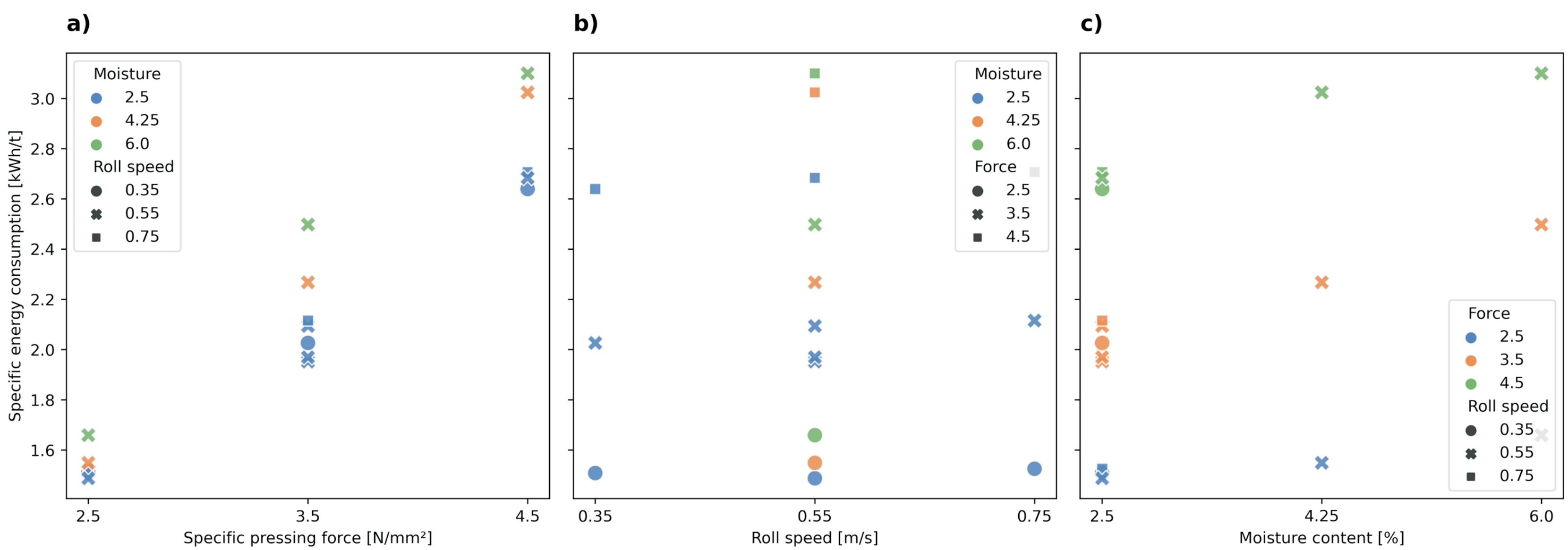

Figure 3. Effect of the operational factors—**a)** specific pressing force, **b)** roll speed, and **c)** moisture content—on the specific energy consumption. Abbreviations: kWh/t, kilowatt-hours per tonne; N, newtons.

power to apply more force. The roll speed does not affect the specific energy consumption. The moisture content has a small impact on the specific energy consumption, indicating that higher moisture content will consume more energy.

Throughput

Figure 4 shows how the three operational factors affect the HPGR throughput. The roller speed highly affects the throughput, which sets the trend. If little or no slippage is assumed at the operating gap (Lim et al., 1997), the particle bed flows at the same speed as the rolls. The specific pressing force also has a significant effect, such that with increasing specific pressing force, the throughput decreases due to the reduction of the operating gap. The moisture content does not significantly influence throughput, but the interaction between the moisture content and specific pressing force is significant. A combination of the specific pressing force and moisture content can be associated with increased slippage at the rolls, leading to a decrease in the throughput.

Specific Throughput

Figure 5 shows the effect of the three operational factors on the specific throughput. The specific throughput (referred to as 'm-dot') is calculated by dividing the throughput by the roll speed, width and diameter, generating a parameter that can be used for scale-up. Due to this, the specific throughput decreases with an increase of the roll speed, indicating that the best performance is not obtained by running the HPGR the fastest. The specific pressing force also leads to a decrease in the specific throughput, so a balance between the best breakage of the material being pressed and the highest throughput must be achieved when optimizing the HPGR operation. The moisture content has an insignificant effect on the specific throughput, but its interaction with the specific pressing force is significant, similar to the results observed with the throughput.

Reduction Ratios of 80% and 50%

Figures 6 and 7 shows the effect of the three operational factors on the reduction ratio for the P_{80} and P_{50} particle sizes, respectively. The only significant factor is the specific pressing force, which is expected. The roll speed and moisture content are not significant. No interactions or quadratic terms were found to be significant for the modelling.

Flake Density

Figure 8 shows the effects of the three operational factors on flake density. The flake density is associated with how compact the material gets as it flows through the rolls. As expected, the specific pressing force plays an important role in increasing the compression and is a significant variable. The interaction of the specific pressing force with the moisture content was also significant. Increasing the moisture content allows an enhancement of compression by reducing the friction between the particles. The roll speed had no significant effect on the flake density.

Flake Thickness

Figure 9 shows how the three operational factors affect the flake thickness. The operating gap is highly correlated to the flake thickness. The flakes serve as a physical indication of the operating gap, with the difference that the flakes expand after being expelled from the rolls. Also, it is important to note that the flake thickness is a manual measurement, subject to higher errors, especially when flakes are uneven. As with the operating gap, the three operational factors had a significant effect on the thickness of the flakes, with the specific pressing force and moisture content having the most significant effect.

Final Models Based on Measured Responses

Table 6 shows the uncoded coefficients for the linear regression equations that serve to predict the responses over the range of the operational factor levels tested, and Table 7 summarizes the fit statistics for the models, including the coefficient of determination (R^2) and standard deviations. The predicted R^2 shows how the model performs when predicting the actual results.

Almost all the models perform very well, with R^2 values of over 0.9, except for the 50% reduction ratio (RR_{50}) and flake density predictions. The poor performance of the 50% reduction ratio is due to the simplicity of the model since it only considers the specific pressing force. Figure 7 shows that although there is a trend of the RR_{50} with the specific pressing force, the dispersion of points for each force level is high, indicating that there has to be another predictor that helps to reduce the prediction error.

The block effect can explain the poor prediction of the flake density. The data is grouped for the tests belonging to blocks 1 and 2, where the flake density is almost the same for all. The data from block 3 deviates from this value due to the change in moisture content. More tests with higher moisture content should be performed to conclude the changes in the modelling. Regardless, the model performs well for low moisture contents, obtaining an error of 0.6%.

Conclusions

This study presents the results of a pilot-scale high-pressure grinding roll test program conducted on ore from the Copper Mountain mine. A 'design of experiments' was performed, which involved varying three operational factors—the specific pressing force, roll speed, and feed moisture content—in 17 tests. Eight responses were recorded during each of the test runs, and for each response, linear regression models were developed, indicating the relative significance of the three operational factors on the eight responses. Operation of the high-pressure grinding roll can

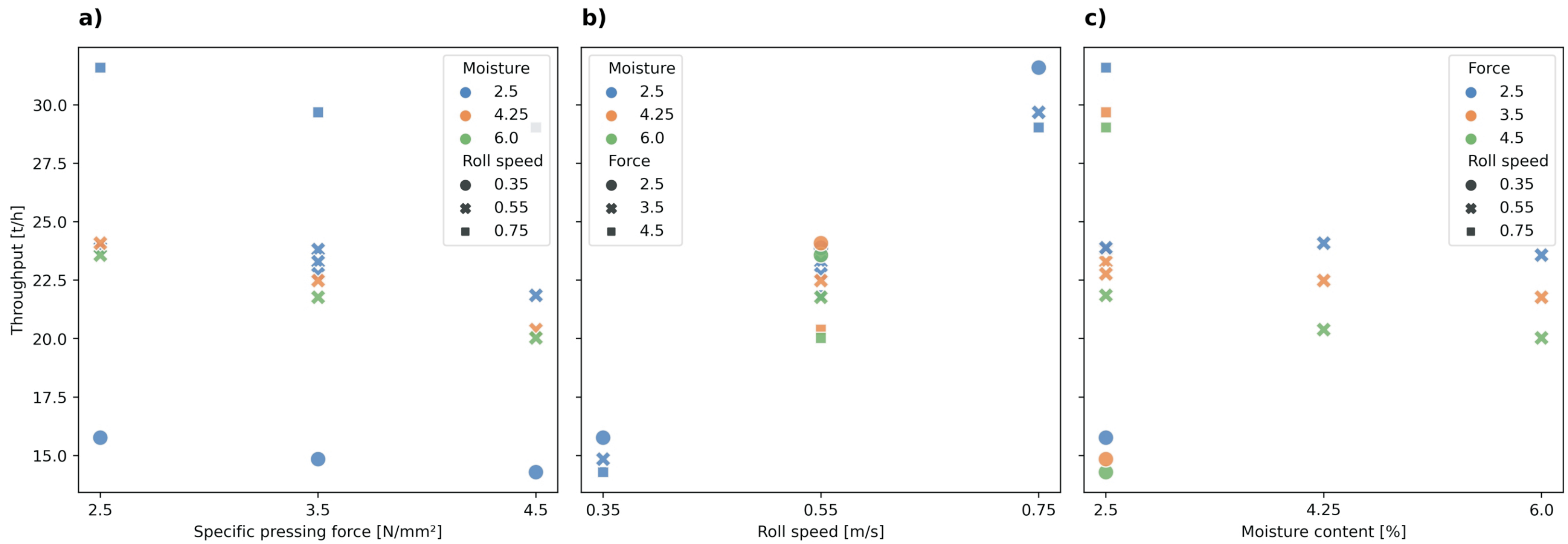

Figure 4. Effect of the operational factors—**a)** specific pressing force, **b)** roll speed, and **c)** moisture content—on the throughput. Abbreviations: N, newtons; t/h, tonnes per hour.

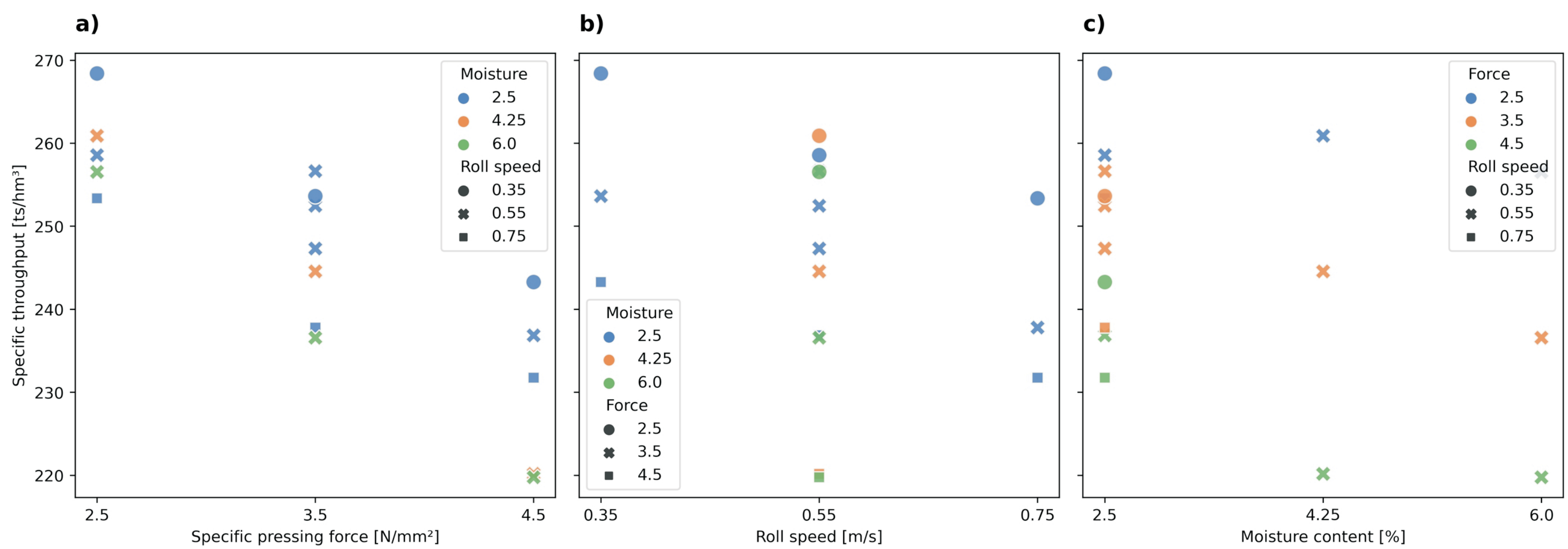

Figure 5. Effect of the operational factors—**a)** specific pressing force, **b)** roll speed, and **c)** moisture content—on the specific throughput. Abbreviations: N, newtons; ts/hm^3, tonnes per hour per cubic metre per second.

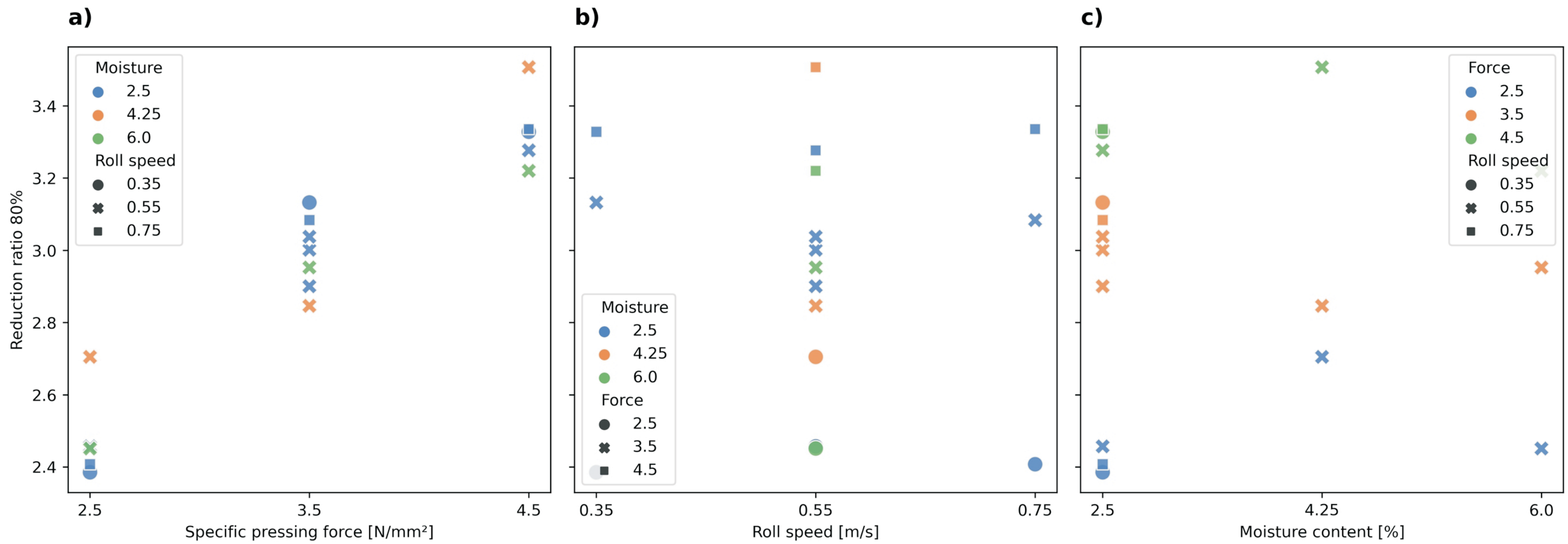

Figure 6. Effect of the operational factors—**a)** specific pressing force, **b)** roll speed, and **c)** moisture content—on the 80% reduction ratio. Abbreviation: N, newtons.

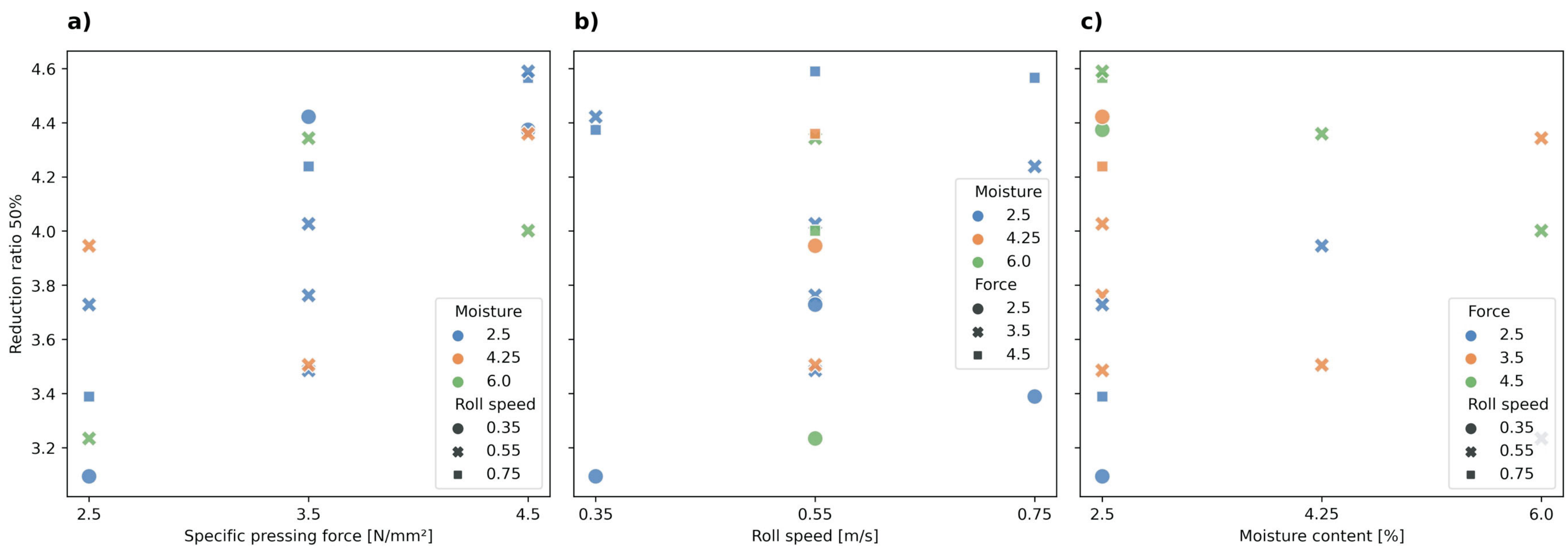

Figure 7. Effect of the operational factors—**a)** specific pressing force, **b)** roll speed, and **c)** moisture content—on the 50% reduction ratio.

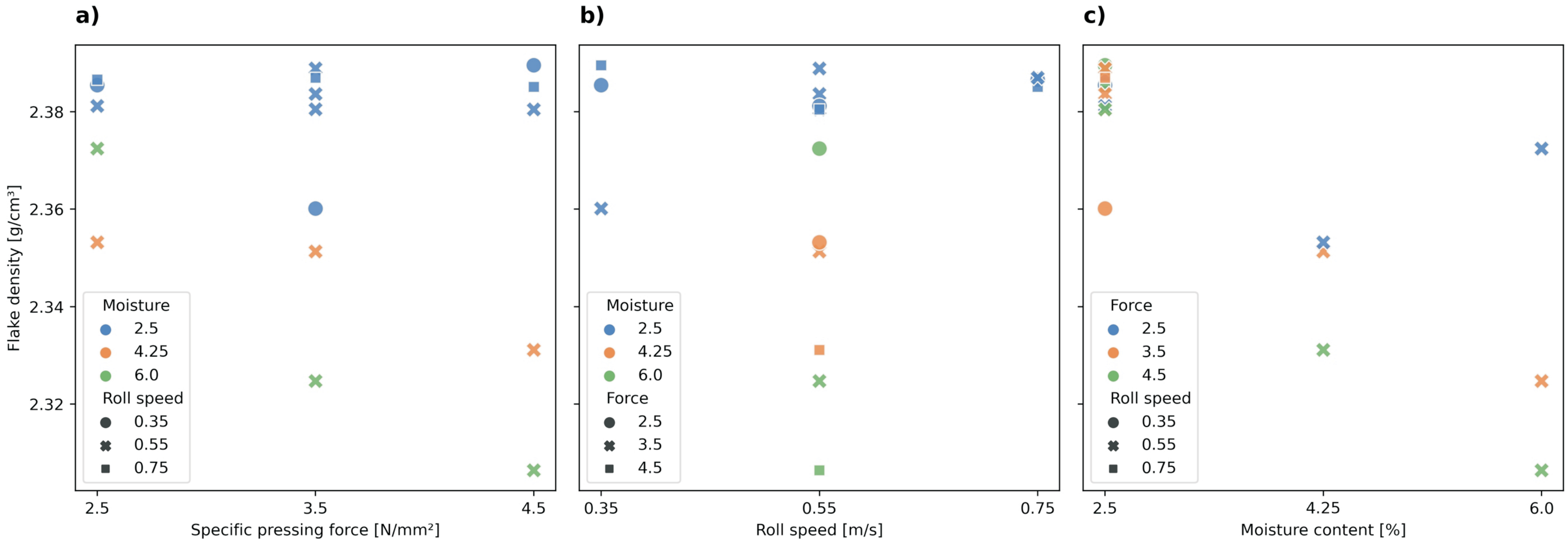

Figure 8. Effect of the operational factors—**a)** specific pressing force, **b)** roll speed, and **c)** moisture content—on flake density. Abbreviation: N, newtons.

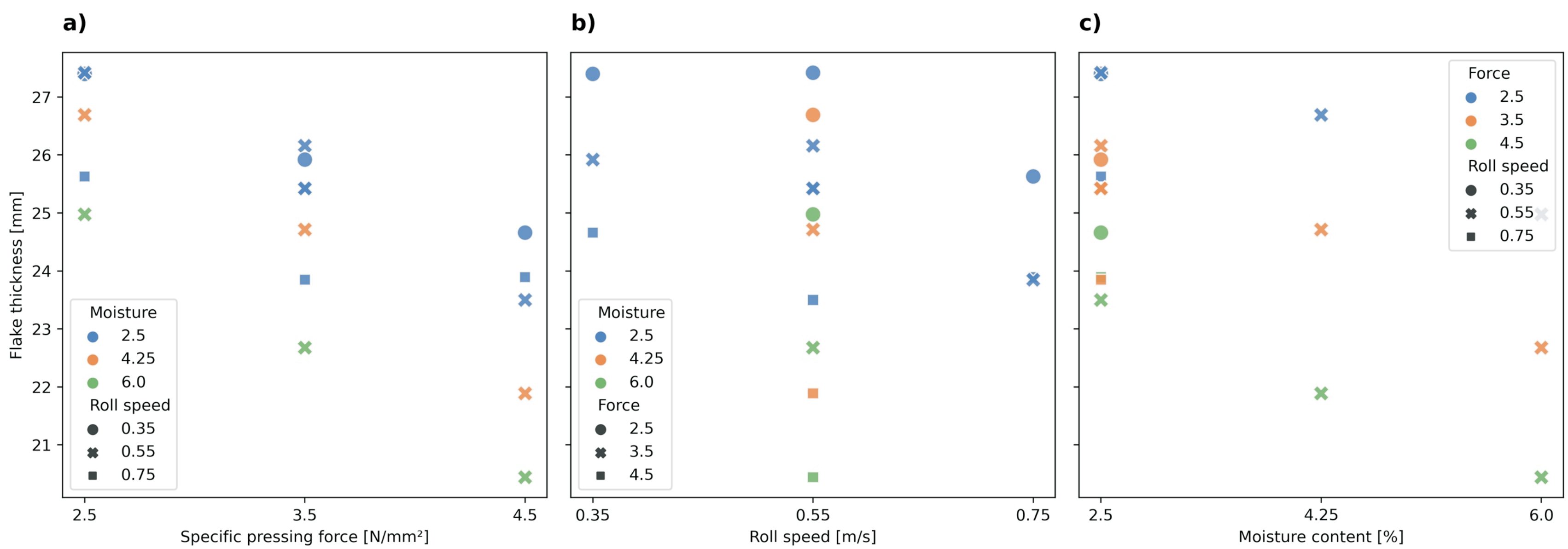

Figure 9. Effect of the operational factors—**a)** specific pressing force, **b)** roll speed, and **c)** moisture content—on flake thickness. Abbreviation: N, newtons.

Table 6. Actual (uncoded) linear regression equations (intercept and coefficients) for the measured responses.

Response	Intercept	Force	Roll speed	Moisture content	Force x moisture content
Operating gap	28.82	-1.51	-2.32	-0.61	
Specific energy consumption	0.2	0.48		-0.08	0.04
Throughput	4.28	-0.45	37.84	0.57	-0.25
Specific throughput	294.7	-6.12	-35.32	5.92	-2.39
Reduction ratio 80%	1.46	0.43			
Reduction ratio 50%	2.41	0.45			
Flake density	2.3	0.02		0.03	-0.01
Flake thickness	36.41	-1.77	-3.84	-0.99	

Table 7. Fit statistics for the linear regression models developed for each of the responses. Abbreviation: R^2, coefficient of determination.

Response	Standard deviation	Mean	Coefficient of variance (%)	R^2	Predicted R^2	Mean absolute error
Operating gap	0.46	20.19	2.3	0.92	0.83	1.60%
Specific energy consumption	0.07	2.17	3.21	0.99	0.96	2.20%
Throughput	0.48	22.54	2.12	0.99	0.98	1.40%
Specific throughput	3.55	245.81	1.44	0.95	0.85	1.00%
Reduction ratio 80%	0.12	2.94	4.11	0.91	0.83	3.40%
Reduction ratio 50%	0.3	3.95	7.52	0.64	0.4	7.20%
Flake density	0.01	2.37	0.34	0.78	0.34	0.60%
Flake thickness	0.64	24.74	2.58	0.9	0.72	2.10%

be optimized using this data to maximize the throughput while minimizing energy consumption to achieve a specific product particle size target. It was found that the best moisture content for the feed was the lowest possible, at 2.5%. Higher moisture contents led to a decrease in throughput and increased energy consumption.

The results of the experimental program revealed that the roll speed only affects the operating gap and throughput, so the breakage and energy consumption should be kept similar when testing other materials from the same deposit. To keep the breakage constant throughout different geometallurgical units, optimizing the pressing force alongside the roll speed is necessary, since it will also affect the throughput. Due to the poor-performing reduction ratio models, it is not possible to make any conclusions on this aspect of the optimization.

This study highlights the importance of conducting pilot-scale tests and experimenting to optimize the operation of a high-pressure grinding roll in mining operations. The results presented can be used as a tool to enhance the efficiency of high-pressure grinding roll operation and reduce operating costs. The models developed in this study can also be extended to other geometallurgical units with similar mineralogical characteristics, such as the ones within the same deposit.

Future work involves prediction of the high-pressure grinding roll response to the same material by using a piston-and-die press test, which utilizes small quantities of material compared to a pilot-scale test. Ongoing research involves using less than 10 kg of material to predict the specific throughput, specific energy consumption, and size reduction of the high-pressure grinding roll. The results presented in this paper are crucial to understanding the behaviour of the high-pressure grinding roll under different factors. This knowledge will be applied in future modelling using a small-scale test.

Acknowledgments

The authors would like to acknowledge M. Westendorf, M. Devicente and I. Atutxa for reviewing the paper, and the staff at the Copper Mountain mine (HudBay Minerals Inc.) and Ingeteam for supporting the research. The lead author would like to thank Geoscience BC for providing financial support through the Geoscience BC Scholarship program.

References

Ghorbani, Y., Mainza, A., Petersen, J., Becker, M., Franzidis, J.P. and Kalala, J. (2013): Investigation of particles with high crack density produced by HPGR and its effect on the redistribution of the particle size fraction in heaps; Minerals Engineering, v. 43–44, p. 44–51, URL <https://doi.10.1016/j.mineng.2012.08.010>.

Lim, W.I.L., Campbell, J.J. and Tondo, L.A. (1997): The effect of rolls speed and rolls surface pattern on high pressure grinding rolls performance; Minerals Engineering, v. 10, p. 401–419, URL <https://doi.10.1016/S0892-6875(97)00017-4>.

Morrell, S. (2022): Helping to reduce mining industry carbon emissions: a step-by-step guide to sizing and selection of energy efficient high pressure grinding rolls circuits; Minerals Engineering, v. 179, art. 107431, URL <https://doi.10.1016/j.mineng.2012.08.010>.

Rashidi, S., Rajamani, R.K. and Fuerstenau, D.W. (2017): A review of the modeling of high pressure grinding rolls; KONA Powder and Particle Journal, v. 34, p. 125–140, URL <https://doi.10.14356/kona.2017017>.

Schönert, K. (1988): A first survey of grinding with high-compression roller mills; International Journal of Mineral Processing, v. 22, p. 401–412, URL <https://doi.10.1016/0301-7516(88)90075-0>.